International Journal of Stem Cell Research and Transplantation (IJST)
ISSN 2328-3548

Human Umbilical Cord Matrix - Derived Stem Cells Show Tropism Towards the Human Glioma Microenvironment

Research article

Abdi Z[1], Eskandary H[2], Nematollahi-Mahani SN[2*]

[1] Faculty of Medicine, Department of Anatomy, Afzalipour School of Medicine, Kerman University of Medical Sciences, Kerman, Iran.
[2] Professor, Department of Anatomy, Afzalipour School of Medicine, Kerman University of Medical Sciences, Kerman, Iran.

Abstract

Objective: Glioblastoma multiforme (GBM) is an aggressive type of brain tumor in humans. The median survival of patients is a year after diagnosis. It is a great challenge to identify new therapeutic strategies that could reach to the tumor mass. A novel approach to this strategy is the use of stem cells. Human umbilical cord matrix-derived mesenchymal cells (hUCM) are an extraordinary source of stem cells for clinical application. In the present study, the aim was evaluating the tropism of hUCM towards the tumor mass and the effects of hUCM inoculation on tumor behavior in an animal model of brain cancer.

Materials and Methods: hUCMs were isolated from Umbilical cord of a normal volunteer. hUCMs were labeled with fluorescent dye and injected into the left ventricle of human glioma-bearing rats. The magnetic resonance imaging, H&E and, Immunohistochemical staining were used to assess characteristics of groups.

Results: hUCMs were found in the tumor bed, but not in the normal parenchyma. H&E and IHC staining data were shown the positive role of hUMCs in inhibition of progression of glioma. In addition; the intracardiac injection was a suitable approach for transplantation of stem cells in brain cancer in comparison with intravascular injection.

Conclusion: Human Umbilical cord matrix-derived mesenchymal cells have the ability of migration towards and homing in GBM tumor. This is important because the hUMCs may be a suitable cellular vehicle for delivery of therapeutic agents to sites of tumor types in human.

Keywords: Cell Migration; Glioblastoma Mutiforme; Human Umbilical Cord Matrix-Derived Mesenchymal Cells; MRI.

Introduction

GBM is a primary malignant brain tumor, which is the most common and aggressive type of brain tumor in humans. Despite improvement in therapy techniques, patients have a short life expectancy (12-15 months) [1-3]. This poor outcome is mainly related to the inability in delivering therapeutic agents to the tumor [4]. It is a great challenge to 1) identify the new therapeutic strategies and agents that could penetrate well through the blood-brain barrier, 2) reach to the tumor mass, and yet cause minimal harm to normal cells [5]. In recent decades, new strategies such as gene therapy have been developed, but gene therapy is confounded by the inefficiencies of viral and adenoviral vectors [6, 7].

Another novel approach is the use of stem cells [8]. Recent evidences suggest that stem cells are capable of migrating to the vicinity of tumor mass [5, 9]. The tropism of stem cells towards the cancerous cells has been reported in many types of cancers such as brain, breast, lung, and ovary tumors [8, 10-14]. Hence, stem cells are great options in the therapy methods of tumors because of their inherent tendency to migrate to the site of injury, ischemia, and tumor [15, 16]. Aboody et al [8] demonstrated the tropism of the neural stem cells into glioma. When NSCs were implanted intracranially, they migrated through the normal parenchyma and the primary tumor bed toward tumor mass and tumor microsatellites. This feature of NSCs led to study the migration behavior of other stem cells in order to develop tumor targeting and therapy strategy by stem cells. Researchers have shown that mesenchymal stem cells are capable of migrating to the tumor cells. Moreover, MSCs are well suited in cell therapy procedures

***Corresponding Author**:
Seyed Noureddin Nematollahi-mahani,
Faculty of medicine, Department of Anatomy, Afzalipour School of Medicine, 22 Bahman Blvd, Kerman, Zip code: 7616914115, Iran.
Tel:+98 9122420037
Fax: +98 3433221671
Email: anatomy1380@gmail.com

Received: November 03, 2015
Accepted: January 05, 2016
Published: January 08, 2016

Citation: Abdi Z, Eskandary H, Nematollahi-Mahani SN (2016) Human Umbilical Cord Matrix - Derived Stem Cells Show Tropism Towards the Human Glioma Microenvironment. *Int J Stem Cell Res Transplant* 04(1), 146-152. **doi:** http://dx.doi.org/10.19070/2328-3548-1600025

because they are easily accessible and can expand in culture [17-19]. In addition, they are capable of differentiating into neurons, astrocytes, and other types of neuronal lineages [20-22].

Human umbilical cord matrix is an extraordinary source of stem cells for clinical applications [23]. Furthermore, hUCMs are easily obtained from delivered offspring, and have the plasticity for differentiation into adipocytes, chondrocytes, osteocytes, and also neuronal lineages [24, 25]. Tropism of hUCMs has been reported in animal models of ischemia and injury [16, 26]. However, no report has shown the migratory capacity of these cells toward the tumor mass. The aim of this study was to evaluate the migration tendency of hUCMs to tumor mass and their effects on tumor progression in an animal model of brain cancer. To assess this, Magnetic Resonance Imaging, H&E, and immunohistochemistry studies have been applied in this study.

Methods and Materials

Collection and Culture of hUCMs

Human umbilical cord was obtained from consented healthy donor. It was delivered to the laboratory in sterile PBS and %1 Penicillin/Streptomycin. The procedure for harvesting hUCMs from umbilical cord was is described previously [27]. Briefly, the matrix was cut into 2-3mm pieces and the pieces were put onto 3 cm petri dishes and culture medium (DMEM, %10 FBS, %1 Penicillin/Streptomycin, 0.0025µg/ml Amphotripcin B) was added. The harvested cells were detached by Trypsin/EDTA and were cultured in 25 cm^2 flasks. The hUCMs from the 3rd passages were used for experiments.

hUCM characterization

Flow cytometry: The method for hUCM cell markers analysis was obtained from Seyedi et al., [28]. Briefly, CD34, CD73, and CD90 markers were evaluated by a FACS Calibur flow cytometer with Cell Quest software (BD Bioscience). Data were analyzed using WinMDI2.9 software.

Adipogenic and Osteogenic differentiation: Adipogenic and osteogenic protocols for differentiation of hUCMs have been described elsewhere [29]. Briefly, 2-3×10^4 viable hUCMs were seeded on clean, sterile coverslips and fed by adipogenic and osteogenic inducing medium for 21 days. Control cells were cultured in convention culture medium without the inducing agents. After 21 days, the Oil-red and Alizarin red staining were used for detection of fat droplets and Calcium-phosphate precipitates in the induced cells.

U87 Cells labeling

U87 cell line was purchased from the Pasteur Institute, Tehran, Iran. The cells were cultured in DMEMF12 with 10% FBS and incubated in a humidified atmosphere at 37ºC with %5 CO_2 in the air. At confluence of %80-90, they were detached from the substratum; counted, and used for the experiments or cryopreserved with 10% DMSO for further use. The PKH_{26} (red dye) was used to label the U87 cells. The cells were labeled according to the manufacture's protocol. For this reason, the cells were trypsinized; centrifuged, counted, and about 10^7 viable cells were exposed to PKH_{26} as recommended by the manufacturer. PKH_{26} positive cells were examined for their fluorescence emission by an inverted microscope equipped with fluorescence apparatus (Olympus, Japan).

Animals

Eighteen male Sprague-Dawley rats weighing 220-250 g were used for the experiments. The rats were housed in the animal room, with 12/12 h day/night cycle, free access to rodents chew and drinking water. They were randomly divided into Tumor, hUCM groups of 7rats, and PBS group of 4 rats.

Implantation of U87-PKH^+_{26} cells

Animals were anesthetized intraperitoneally using a mixture of 100 mg/kg ketamine and 10 mg/kg xylazine. Head of the animals got shaved and fixed in a stereotaxic frame. The scalp was incised in the midline of the skull. A hole with the coordinate; anterior = 1mm, lateral = 2mm of the Bergma was drilled in the right half of the skull. The Hamilton syringe was fixed on the arm of the stereotaxic frame. For tumor and hUCM groups, the needle was inserted to the depth of 3-4 mm, and 10 µl of cell suspension (10^6 cells) was injected slowly (1µl/1min). After 5 minutes, the needle was withdrawn gently. The hole was covered with bone wax and the incision was sutured with 0-4 suture. The same procedure was carried out for PBS group, except that the cells were removed.

Determination of tumor by MRI

MRI was performed on the animals 10 days after tumor inoculation. The animals were anesthetized by intraperitoneal injection of ketamine and xylazine. The rats were positioned head-up in the knee coil of 1.5-Tesla unite (AVAN TO Siemens imaging system, Germany), and T1-weighted spin-echo images (TR= 400 ms, TE= 19 ms, slice thickness=2 mm), T2-weighted spin-echo images (TR= 2000 ms, TE= 72 ms, slice thickness=2 mm) were obtained.

hUCM transplantation

hUCM cells were injected into the heart of the hUCM group animals, 10 days after implantation of tumor. To visualize transplanted cells, PKH_{67} (green dye) was used for labeling as recommended by manufacturer. The animals were anesthetized with ketamine/xylazine; the skin of the thorax was shaved, and a 1cm oblique incision was made in the left half; 2 cm lateral to the midline. The pectoralis major and external intercostal muscles were cut in the fifth intercostal space. Afterward, 2×10^6 hUCM-PKH_{67}^+ cells suspended in 100 µL PBS was injected into the left ventricular by insulin syringe. Injections were done manually over 3 minutes, and the incision was sutured with 0-4 suture. 17 days after implantation of tumor, the rats were anesthetized, and were perfused with 4% paraformaldehyde. The brains were post-fixed by 10% buffered formalin for 24 h and were immersed in 30% sucrose in PBS for 48 h.

H & E and Immunohistochemistry Staining

For Hematoxylin-Eosin and immunohistochemical staining, formalin-fixed, paraffin-embedded 3µm tissue sections were mounted on Plus slides. Following deparaffinization and rehydra-

tion, numbers of sections were incubated with primary antibodies as follows; monoclonal mouse anti-human Ki-67; 1:100 (Dako, Carpinteria, CA), monoclonal mouse anti-human Nestin; 1:100 (Santa Cruz Biotechnology), PECAM-1 monoclonal mouse anti-rat CD31; 1:100 (a Bio-Rad), monoclonal mouse anti- human antibody GFAP; 1:100 (Santa Cruz Biotechnology) all diluted in PBS. Slides were incubated with biotinylated secondary antibodies against rat and rabbit followed by incubation with the streptavidin and biotinylated peroxidase complex (Dako REAL™ EnVision™ Detection System, Peroxidase/DAB, Rabbit/Mouse). Sections were counterstained with hematoxylin and mounted by a coverslip. The proportion of Ki-67, GFAP, CD-31, and Nestin positive cells was calculated as the percentage of the stained cells in 200 cells. Some of the sections were stained with H&E for histologic evaluation of tumors.

To detect PKH^+ cells in the brain tissue, the brains (n=3) was immediately frozen in Tissue-Tek OCT embedding gels. Cryostat-generated 8-10 μm sections were mounted onto Superfrost Plus slides (Fisher) and examined under a fluorescence microscope (IX 71, Olympus, Japan) equipped with a digital camera.

Statistical Analysis

Data are expressed as mean ± SEM. Distribution of data was analyzed by the Kolmogorov-Smirnov test. Statistical differences were analyzed with the use of one way ANOVA test with IBM SPSS Statistics version 21. A P value < 0.05 was considered to detect a statistically significant difference.

Results

hUCM characterization

Flow cytometric analysis revealed that hUCM cells were positive for the typical mesenchymal markers CD73 and CD90, but negative for the hematopoietic marker CD34 (Figure 1 A). The induced hUCMs were capable of differentiating into osteocytes (Figure 1 B) and adipocytes (Figure 1 C) lineages.

MRI

MRI was performed in groups to assess cerebral injury and tumor development. It also performed on the 10th day of experiments using T1 and T2-weighted MRI without contrast enhancement.

On T2-W, images a hyperintense spot was detected in the white matter of the right frontal lobe without obvious damage. On coronal T1-W images, the spot was iso- to hypointense in the tumor groups. Any sign of cerebral injury like edema, cyst formation and hemorrhage were observed in the animals of the tumor and PBS groups (Figure 2 A and B).

Histopathology

To assess whether transplanted hUCM cells could migrate towards the tumor mass frozen serial sections were examined with a fluorescence microscope. Tumor area was clearly seen in the slides (Figure 3 A-B). hUCM-PKH_{67}^+ cells were detectable inside and vicinity the tumor mass (Figure 3 C-D). Normal parenchyma far from the tumor was devoid of any detectable fluorescence signals.

H & E staining in U87 inoculated animals revealed that glioma masses were stained strongly with hematoxylin in compared with the normal parenchyma. The presence of neoplastic characteristics such as mitotic activity, migration of tumor cells, neovascularization, necrotic clusters, pseudopalisading cells, and hemorrhage was observed in tumor and hUCM groups (Figure 4 A-B). Interestingly, hemorrhage was very intense in hUCM treated animals compared with the tumor group (Figure 4 B). In PBS group, infiltration of immune system cells, and dead blood cells were observed in the injection area (Figure 4 C). For neo-vascularization

Figure1. A-Flow cytometry analysis of hUCM cells. Red histograms display the isotype control-stained cells, and the black histograms show the antibody stained. B- Oil red staining exhibited lipid droplets in the cytoplasm of the induced cells. C-Alizarin red staining, displayed Ca^{2+} aggregation in the extracellular matrix of induced cells.

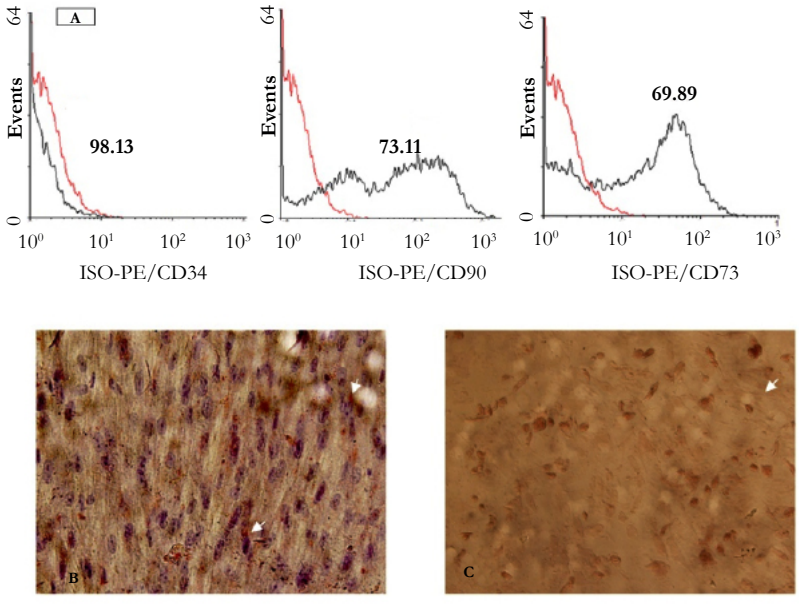

Figure 2. A, B- The magnetic resonance images of both groups.

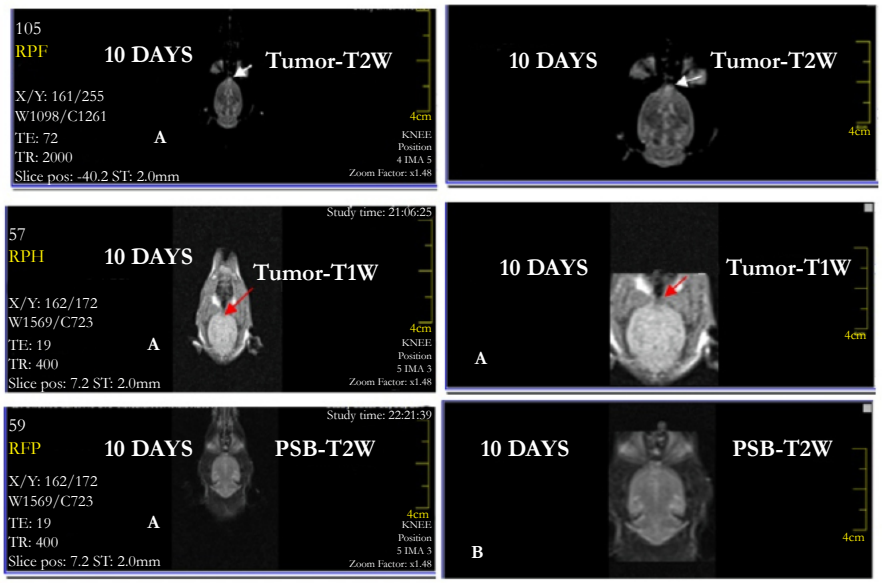

Figure 3. Frozen sections of tumoral tissues were shown in the groups of tumor implantation A, B– Frozen sections were seen with green filter for tracking PKH-26 positive tumor cells. Frozen sections were counterstained with hoechst. Merge of images for detection of areas of tumor ×200. C. Frozen sections were seen with blue filter for tracking PKH-67 positive hUM cells. Frozen sections were counterstained with hoechst. Merge of images for detection of PKH-67 positive hUM cells ×200. D. Merge of the frozen sections of hUMC group that were seen with green and blue filter. E. Frozen sections were seen with blue filter for tracking PKH-67 positive hUM cells in the vicinity of tumor mass. Frozen sections were counterstained with hoechst. Merge of images for detection of PKH-67 positive hUM cells in the vicinity of tumor mass ×200.

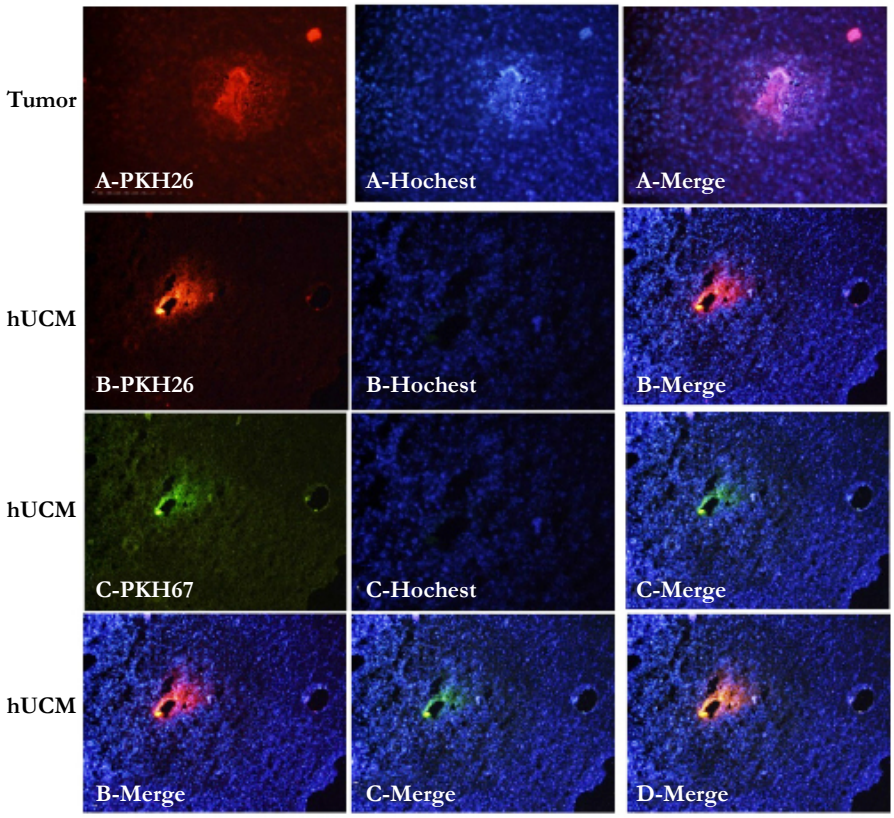

determination, 10 H & E sections were investigated randomly, and new vessels were counted at 200 magnification. No significant difference was found between the hUCM and tumor groups in angiogenesis. While, both groups had statistically significant difference with the PBS group (Figure 4 D-F and 5 A).

Immunohistology

GFAP: GFAP positive cells were present in all groups (Figure 6 A-C). Interestingly, GFAP expression was lower in hUCM group, and depicted a significant difference with other groups. The rate of GFAP positive cells was significantly lower in the PBS group than in the tumor group (Figure 5-B).

Ki-67: The proportion of Ki-67 positive cells in the tumor group was significantly higher than other groups (P< 0.01, Figure 5-B). In addition, hUCM group had significantly higher Ki-67 positive cells than the PBS group. The increase of the Ki-67 positive cells revealed an increase in mitotic activity in tumor mass (Figure 6 D-F).

Nestin: The rate of Nestin positive cells was 9.75% in the tumor group. That it was significantly higher than other groups (Figure 5-B). There was also no significant difference between the PBS and hUCM group (Figure 6 G-I).

CD-31: The tissues of the tumor group exhibited more than %5 CD31 immunostained cells (Figure 5-B). It was also detectable in hUCM group, but no statistical difference was observed between the groups (Figure 6 J-K).

Discussion

Human umbilical cord matrix-derived mesenchymal cells (hUCM) have been recognized for their capacity to differentiation into a neural phenotype *in vitro* [23]. Transplanted hUCMs showed remarkable ability to migrate toward pathological areas such as ischemia and injury [16, 26, 30]. Recently, evidences have shown the ability of hUCMs in wound healing after spinal cord injury [31]. We could show the potential of hUCMs migration toward the tumor area and their positive role in tumor regression. The surface makes analysis of hUCMs and their ability to differentiate into adipogenic and osteogenic lineages showed their mesenchymal origin and potential, which was consistent with the previous studies [28, 29]. MRI was employed for determination of tumor in the brain of animals. Tumor growth was monitored by 1.5 Tesla MRI system, and the tumor mass was observed 10days after tumor-implantation. Obtained data were similar to the other reported data by using 1.5 T MRI systems [32].

Specifically, after intravascular injection of hUCMs, the migration of hUCMs in tumor-bearing rats was investigated. The results showed the weak presence of hUCMs in the tumor area. Their data are in agreement with the data presented by other researchers, who found low tropism of human mesenchymal stem cell in

Figure 4. H&E sections of groups. A- The area of tumor in the tumor group (black arrow) × 100. B- The area of tumor in the hUMC group with hemorrhage (black arrow) × 100. C- Injection site of PBS (black arrow) ×100. D- Angiogenesis in tumor mass in the tumor group (black arrow) × 200. E-Angiogenesis in tumor mass in the hUMC group (black arrow) × 200. F- Angiogenesis in injection site of PBS in the PBS group (black arrow) × 200.

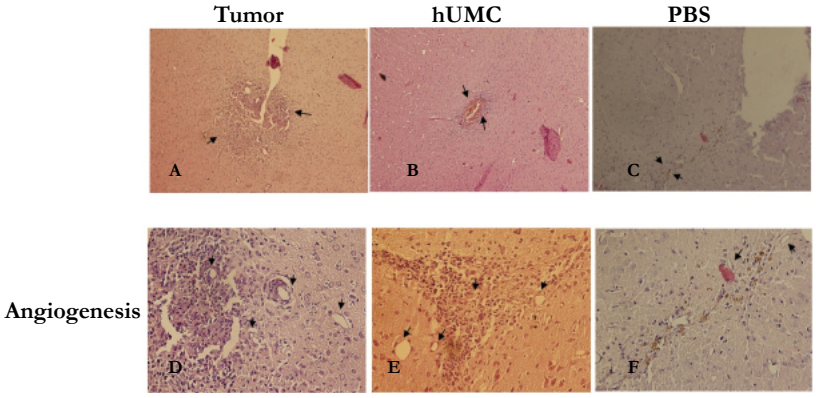

Figure 5. A- Angiogenesis analysis between groups. B- Immunohistology analysis of Nestin, CD-31, Ki-67, and GFAP in groups. Data are expressed as mean ± SEM. *P < 0.05, **< 0.01.

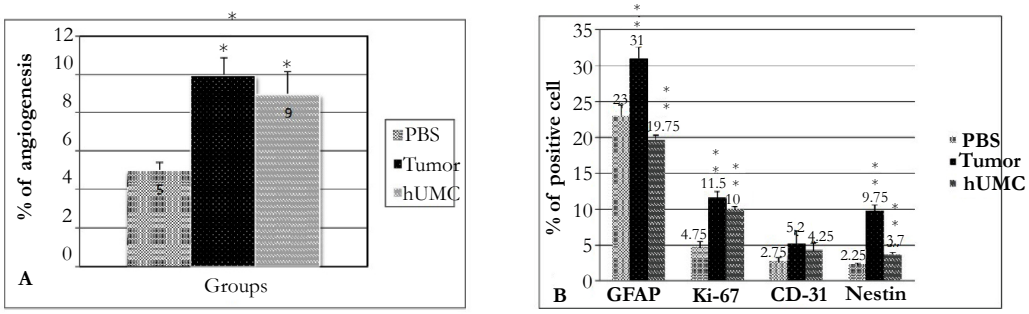

Figure 6. Immunostaining of groups. A- GFAP positive tumor cell in the tumor area in the tumor group (black arrows) × 200. B- GFAP positive tumor cell in the tumor area in the hUMC group (black arrows) × 100. C- GFAP positive cells in the PBS group (black arrows) × 200. D- Ki-67 positive tumor cell in the tumor area in the tumor group (black arrows) ×320. E- Ki-67 positive tumor cell in the tumor area in the hUMC group (black arrows) × 200. F- Ki-67 positive tumor cell in were present in the site of injection in the PBS group (black arrow) × 200. G- Nestin positive tumor cell in the tumor area in the tumor group (black arrows) × 320. H- Nestin positive tumor cell in the tumor area in the hUMC group (black arrows) ×320. I- Nestin in PBS group; a few Nestin positive were detected in the injection area (black arrows) × 200. J- CD-31 positive cells in tumor area in the tumor group (black arrows) ×200. K- CD-31 positive cells in tumor area in the hUMC group (black arrows) × 200.

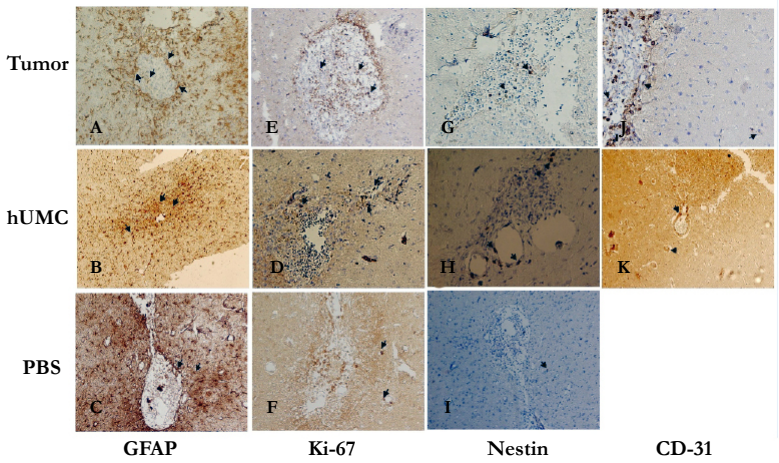

the tumor area after cell transplantation via tail vein injection [8, 33]. Our primary results (data not shown) indicated that via tail vein injection was not a suitable approach for migration of stem cells towards tumor mass, thus, we switched to another method of cell inoculation, which uses intracardiac route. We found that hUCMs specifically localized in the tumor mass, but not in the normal brain. Thus, our results suggested homing of hUCMs is not merely the result of cerebral blood flow patterns, rather is due to the inherent tendency of hUCMs for the tumor. Reports indicated that the tropism of stem cells toward tumor may be mediated by tumor microenvironment, because the tumor's milieu expresses EGF, PDGF, FGF, and SDF-1a which EGF, PDGF, and SDF-1 enhanced migration of stem cells toward tumor [34-36].

Analysis of histological slides of the brain revealed a similar histopathological characteristic of human glioblastoma such as polymorphism, mitotic activity, invasion, necrosis, hemorrhage, and neoangiogenesis [3] in tumor and hUCM groups. In this study, Ki-67 antigen expression indicated that the proliferation of U87 cells was decreased in the hUCM group, which suggested the role of hUCM in the inhibition of tumor progression. Moreover, the rate of neoangiogenesis and the expression rate of CD31 were decreased in the hUCM group in comparison with the Tumor group, however no statistical difference was found between them. Thus, it can be concluded that the presence of hUCMs in the tumor mass had negative effects on tumor growth and led to inhibit of progression of glioma. Some reports confirmed the role of stem cells in the inhibition of tumor progression and angiogenesis [33, 37, 38]. While, some researchers reported that the presence of mesenchymal stem cells in tumor area led to further growth and increased rate of angiogenesis in the tumor [39].

Recently, the expression rate of Nestin has been used as a marker to determine GBM prognosis in cancerous patients. Nestin is usually expressed in the primary brain tumor as well as some areas in the brain such as subventricular zone [40]. Our data showed Nestin expression in tumor mass and periphery in tumor and hUCM groups. In addition, we observed a decreased expression of GFAP in the treated rats. However, the expression rate of GFAP in glioma-bearing rats was very intense in the borders of the tumor as reported earlier [41]. Interestingly, the decrease in GFAP expression was observed in hUCM group, which might be because of the low synthesis of GFAP after migration of hUCM toward glioma. Our IHC staining data indicated the positive role of hUCMs in the inhibition of tumor progression and angiogenesis. Nevertheless, more investigations about 1) the mechanisms of hUCMs migration to the tumor site, 2) the mechanisms of hUCMs in the inhibition of tumor progression and 3) the final fate of hUCMs after the migration toward tumor mass is needed.

Conclusion

The present study suggests that the human umbilical cord matrix-derived stem cells have the ability of migration toward glioma mass. In fact, this is the first demonstration that human umbilical cord matrix-derived stem cells can penetrate through the blood-brain barrier, and reach to the human glioma. This is important because the hUMCs may be a suitable cellular vehicle for delivery of therapeutic agents to sites of tumor types in human. In addition; our work suggests that the intracardiac injection was a suitable approach for transplantation of stem cells in brain cancer in comparison with intravascular injection.

References

[1]. Black PM (1991) Brain tumor. N Engl J Med 324(22): 1555-1564.
[2]. Adamson C, Kanu OO, Mehta AI, Di C, Lin N, et al. (2009) Glioblastoma multiforme: a review of where we have been and where we are going. Expert Opin Investig Drugs 18(8): 1061-1083.
[3]. Lacroix M, Abi-Said D, Fourney DR, Gokaslan ZL, Shi W, et al. (2001) A multivariate analysis of 416 patients with glioblastoma multiforme: prognosis, extent of resection, and survival. J Neurosurg 95(2): 190-198.
[4]. Jansen M, de Witt Hamer PC, Witmer AN, Troost D, van Noorden CJ

(2004) Current perspectives on antiangiogenesis strategies in the treatment of malignant gliomas. Brain Res Rev 45(3): 143-163.
[5]. Dirks PB (2001) Glioma migration: clues from the biology of neural progenitor cells and embryonic CNS cell migration. J Neurooncol 53(2): 203-212.
[6]. Hwang DH, Jeong SR, Kim BG (2011) Gene transfer mediated by stem cell grafts to treat CNS injury. Expert Opin Biol Ther 11(12): 1599-1610.
[7]. Conget PA, Minguell JJ (2000) Adenoviral-mediated gene transfer into ex vivo expanded human bone marrow mesenchymal progenitor cells. Exp Hematol 28(4): 382-390.
[8]. Aboody KS, Brown A, Rainov NG, Bower KA, Liu S, et al. (2000) Neural stem cells display extensive tropism for pathology in adult brain: evidence from intracranial gliomas. Proc Natl Acad Sci U S A 97(23): 12846-12851.
[9]. Ehtesham M, Kabos P, Gutierrez MA, Chung NH, Griffith TS, et al. (2002) Induction of glioblastoma apoptosis using neural stem cell-mediated delivery of tumor necrosis factor-related apoptosis-inducing ligand. Cancer Res 62(24): 7170-7174.
[10]. Sasportas LS, Kasmieh R, Wakimoto H, Hingtgen S, van de Water JA, et al. (2009) Assessment of therapeutic efficacy and fate of engineered human mesenchymal stem cells for cancer therapy. Proc Natl Acad Sci U S A 106(12): 4822-4827.
[11]. Sonabend AM, Ulasov IV, Tyler MA, Rivera AA, Mathis JM, et al. (2008) Mesenchymal stem cells effectively deliver an oncolytic adenovirus to intracranial glioma. Stem Cells 26(3): 831-841.
[12]. Dwyer RM, Ryan J, Havelin RJ, Morris JC, Miller BW, et al. (2011) Mesenchymal Stem Cell-Mediated Delivery of the Sodium Iodide Symporter Supports Radionuclide Imaging and Treatment of Breast Cancer. Stem Cells 29(7): 1149-1157.
[13]. Kanehira M, Xin H, Hoshino K, Maemondo M, Mizuguchi H, et al. (2007) Targeted delivery of NK4 to multiple lung tumors by bone marrow-derived mesenchymal stem cells. Cancer Gene Ther 14(11): 894-903.
[14]. Serakinci N, Christensen R, Fahrioglu U, Sorensen FB, Dagnæs-Hansen F, et al. (2011) Mesenchymal stem cells as therapeutic delivery vehicles targeting tumor stroma. Cancer Biother Radiopharm 26(6): 767-773.
[15]. Chan JKY, Lam PYP (2013) Human mesenchymal stem cells and their paracrine factors for the treatment of brain tumors. Cancer Gene Ther 20(10): 539-543.
[16]. Choi YH, Kurtz A, Stamm C (2011) Mesenchymal stem cells for cardiac cell therapy. Hum Gene Ther 22(1): 3-17.
[17]. Hall B, Dembinski J, Sasser AK, Studeny M, Andreeff M, et al. (2007) Mesenchymal stem cells in cancer: tumor-associated fibroblasts and cell-based delivery vehicles. Int J Hematol 86(1): 8-16.
[18]. Klopp AH, Spaeth EL, Dembinski JL, Woodward WA, Munshi A, et al. (2007) Tumor irradiation increases the recruitment of circulating mesenchymal stem cells into the tumor microenvironment. Cancer Res 67(24): 11687-11695.
[19]. Studeny M, Marini FC, Dembinski JL, Zompetta C, Cabreira-Hansen M, et al. (2004) Mesenchymal stem cells: potential precursors for tumor stroma and targeted-delivery vehicles for anticancer agents. J Natl Cancer Inst 96(21): 1593-1603.
[20]. Lou J, Xu F, Merkel K, Manske P (1999) Gene therapy: adenovirus-mediated human bone morphogenetic protein-2 gene transfer induces mesenchymal progenitor cell proliferation and differentiation in vitro and bone formation in vivo. J Orthop Res 17(1): 43-50.
[21]. Caplan AI, Bruder SP (2001) Mesenchymal stem cells: building blocks for molecular medicine in the 21st century. Trends Mol Med 7(6): 259-264.
[22]. Tocci A, Forte L (2003) Mesenchymal stem cell: use and perspectives. Hematol J 4(2): 92-96.
[23]. Can A, Karahuseyinoglu S (2007) Concise Review: Human Umbilical Cord Stroma with Regard to the Source of Fetus-Derived Stem Cells. Stem cells 25(11): 2886-2895.
[24]. Forraz N, McGuckin CP (2011) The umbilical cord: a rich and ethical stem cell source to advance regenerative medicine. Cell Prolif 44(Suppl 1): 60-69.
[25]. Gang E, Jeong J, Han S, Yan Q, Jeon C, et al. (2006) *In vitro* endothelial potential of human UC blood-derived mesenchymal stem cells. Cytotherapy 8(3): 215-227.
[26]. Harting MT, Baumgartner JE, Worth LL, Ewing-Cobbs L, Gee AP, et al. (2008) Cell therapies for traumatic brain injury. Neurosurg Focus 24(3-4): E18.
[27]. Salehinejad P, Alitheen NB, Nematollahi-Mahani SN, Ali AM, Omar AR, et al. (2012) Effect of culture media on expansion properties of human umbilical cord matrix-derived mesenchymal cells. Cytotherapy 14(8): 948-953.
[28]. Seyedi F, Farsinejad A, Moshrefi M, Nematollahi-Mahani SN (2015) *In vitro* evaluation of different protocols for the induction of mesenchymal stem cells to insulin-producing cells. In Vitro Cell Dev Biol Anim 51(8): 866-878.
[29]. Kaviani M, Ezzatabadipour M, Nematollahi-Mahani SN, Salehinejad P, Mohammadi M, et al. (2014) Evaluation of gametogenic potential of vitrified human umbilical cord Wharton's jelly–derived mesenchymal cells. Cytotherapy 16(2): 203-212.
[30]. Wise AF, Williams TM, Kiewiet MB, Payne NL, Siatskas C, et al. (2014) Human mesenchymal stem cells alter macrophage phenotype and promote regeneration via homing to the kidney following ischemia-reperfusion injury. Am J Physiol Renal Physiol 306(10): F1222-F1235.
[31]. Yang CC, Shih YH, Ko MH, Hsu SY, Cheng H, et al. (2008) Transplantation of human umbilical mesenchymal stem cells from Wharton's jelly after complete transection of the rat spinal cord. PloS One 3(10): e3336.
[32]. Vince GH, Bendszus M, Schweitzer T, Goldbrunner RH, Hildebrandt S, et al. (2004) Spontaneous regression of experimental gliomas-an immunohistochemical and MRI study of the C6 glioma spheroid implantation model. Exp Neurol 190(2): 478-485.
[33]. Nakamizo A, Marini F, Amano T, Khan A, Studeny M, et al. (2005) Human bone marrow–derived mesenchymal stem cells in the treatment of gliomas. Cancer Res 65(8): 3307-3318.
[34]. Bissell MJ, Radisky D (2001) Putting tumours in context. Nat Rev Cancer 1(1): 46-54.
[35]. Coussens LM, Werb Z (2002) Inflammation and cancer. Nature 420(6917): 860-867.
[36]. Nakamura K, Ito Y, Kawano Y, Kurozumi K, Kobune M, et al. (2004) Antitumor effect of genetically engineered mesenchymal stem cells in a rat glioma model. Gene Ther 11(14): 1155-1164.
[37]. Eskandary H, Basiri M, Nematollahi-Mahani SN, Mehravaran S (2011) The role of stem cells in tumor targeting and growth suppression of gliomas. Biologics 5: 61-70.
[38]. Ho IA, Toh HC, Ng WH, Teo YL, Guo CM, et al. (2013) Human bone marrow-derived mesenchymal stem cells suppress human glioma growth through inhibition of angiogenesis. Stem cells 31(1): 146-155.
[39]. Lin G, Yang R, Banie L, Wang G, Ning H, et al. (2010) Effects of transplantation of adipose tissue-derived stem cells on prostate tumor. Prostate 70(10): 1066-1073.
[40]. Ehrmann J, Kolář Z, Mokrý J (2005) Nestin as a diagnostic and prognostic marker: immunohistochemical analysis of its expression in different tumours. J Clin Pathol 58(2): 222-223.
[41]. Yusubalieva GM, Baklaushev VP, Gurina OI, Tsitrin EB, Chekhonin VP (2010) Immunochemical analysis of glial fibrillary acidic protein as a tool to assess astroglial reaction in experimental C6 glioma. Bull Exp Biol Med 149(1): 125-130.